The Influence of Magnitude and Rise Time of Applied Voltage and the Type of Oil on Streamer Growth in a Wet-Mate DC Connector

Mona Ghassemi[1], Qin Chen[2] and Yang Cao[1,3]
[1]Electrical Insulation Research Center, Institute of Materials Science, University of Connecticut,
97 North Eagleville Road, Storrs, CT 06269-3136, USA
[2]GE Global Research Center, Niskayuna, NY 12309, USA
[3]Electrical and Computer Engineering, University of Connecticut
371 Fairfield Way, Storrs, CT 06269-4157, USA

ABSTRACT

For the safe design and operation of wet-mate (WM) DC power connector, a time-dependent full thermo-electrodynamic model comprised of Poisson's equation, three charge continuity equations-one each for the positive and negative ions and one for the electrons-, and a thermal diffusion equation is developed to study the streamer initiation and propagation in the oil portion of a WM DC chamber. The electric field dependent molecular ionization mechanism accounts for the source term for free charge carriers, and positive ion/electron recombination, positive/negative ion recombination and electron attachment represent sink terms in the oil section. The solid portion of the WM DC connector is modeled as a perfect insulator. Considering a needle-sphere electrode geometry with electrodes covered by a dielectric solid and oil enclosed by the dielectric solid, it is approached the complicated solid-liquid insulation system envisaged in a WM DC connector after mating. By using the model, the influence of three parameters including magnitude and rise time of applied voltage as well as the type of oil on streamer initiation and propagation is investigated. It is found that the shorter rise time the more prominent streamer growth in the oil portion. For oil comprising only aromatics, an electric field magnitude larger than about 2×10^8 V/m is needed to propagate streamers, while this value for the oil comprising naphthenics/paraffinics will be exceeding 4×10^8 V/m.

Index Terms — **Polarity, amplitude and rise time of applied voltage, type of oil, streamer propagation, solid-liquid insulation system, wet-mate DC connector.**

1 INTRODUCTION

DUE to the remote and harsh environment, oil and gas production by offshore drilling is more challenging than land-based installation. In addition, diminishing oil and gas reservoirs in existing Brownfield sites cause offshore drilling activity to continue to migrate into Greenfield sites located in deeper water and further away from the shore. Offshore drilling is growing rapidly beyond conventional oil platforms and expanding towards a standalone subsea system for technical and economic reasons.

Since the use of AC subsea transmission and distribution system to supply subsea process in the mentioned Greenfield sites becomes impractical once beyond the critical length limit of AC submarine cables due to their capacitive charging current, a modular stacked DC (MSDC) subsea transmission and distribution system [1-3] emerges as a promising technology alternative.

Manuscript received 18 November 2016, in final form 3 March 2017, accepted 7 March 2017. Corresponding author: M. Ghassemi.

Allowing only the faulty module to be retrieved for repair, wet-mate (WM) DC connectors are key to the reduction of downtime for the complete MSDC system [4]. Although subsea AC connectors are already commercially available and have entered field application with voltage rating up to 36 kV for wet-mate and 145 kV for dry-mate [5, 6], currently there is no commercially available wet-mate DC power connector.

Two designs are currently available for mating of WM connectors: 1) conventional stab type connector with exposed contact pins; and 2) environmental friendly type connectors. One representative design of the latter is the 36-kV/500-A WM AC connector known as MECON [5, 7] where the two halves of the connector are first robotically connected with seawater enclosed in the WM chamber. The chamber is then flushed several times with a) high velocity sea water to remove particles, b) fresh water to desalt, and c) ethanol, respectively. Eventually the chamber is filled with dielectric oil to provide electrical insulation, and then a moving metal contact is engaged to establish electrical connection capable of carrying high current. Since it is very difficult to remove all seawater

DOI: 10.1109/TDEI.2017.006448

molecules containing dissolved salt (sodium chloride) and other minor ionic species from the chamber, there are still residual moisture and ions in the dielectric liquid even after mating and during normal operation [8]. Such "clean environment" design has been adopted for the development of WM DC connector. In this paper, this type of design is considered.

A WM DC connector shall operate under both steady state and switching transient conditions in a corrosive environment for high reliability and minimum maintenance through its lifetime. There is no standard specifically dealing with the requirements for WM DC connector testing. In this regard, CIGRE Electra 189 [9] and CIGRE TB496 [10] are the only existing recommendations for testing the land and submarine HVDC cables. IEC 62895 [11] is still under preparation. A feasibility study on using the aforementioned testing methods for WM DC connectors was reported in [12] where gaps between the existing test recommendations and requirements for WM DC connectors were identified. It should be noted that hybrid solid-liquid insulation geometries in a WM DC connector after mating do not exist in extruded HVDC cables. Therefore, compliance with CIGRE recommendations and IEC standards may not be sufficient for them. Even with the future development of international standards and recommendations applicable for WM DC connectors, the required tests such as load cycle, high load, polarity reversal, superimposed impulse with same and opposite polarities, and DC withstand for the WM DC connectors, along with the cable, will need the cutting-edge high voltage laboratory facilities for testing at 1.45-2.5U_0 where U_0 is the service voltage. Such tests in particularly the superimposed impulse tests are extremely complex and expensive.

In contrast, despite the needs of further improvement [13], there is a growing trend in numerical modeling of fast dynamic phenomena which may result in the streamer formation and the eventual electrical breakdown in gas or liquid insulated systems subjected to transient surges. Benefitting greatly from more robust and faster computational solver algorithm, higher performance computing, high fidelity multiphysics modeling toolboxes are emerging as indispensable development tool for high voltage engineers. While physical test validation is still needed, the development cycle for complicated HV components like WM DC connectors can be significantly reduced.

In this regard, a time-dependent full electrodynamic model comprised of Poisson's equation, three charge continuity equations-one each for the positive and negative ions and one for the electrons, was developed in [14] to study the streamer initiation and propagation in the oil portion of a WM DC connector. Three mechanisms may lead to the increase of the free charge carrier concentration in a dielectric liquid when highly electrically stressed. They are 1) charge injection or Fowler-Nordheim charge injection from the cathode [15-17], 2) Electric field dependent ionic dissociation [18-21], and 3) Electric field dependent molecular ionization [22-24].

Based on studies presented in [25-27] neither Fowler-Nordheim charge injection nor electric field dependent ionic dissociation is considered the dominant mechanism in streamer initiation and growth in transformer oil. The simulation results generated using the full electric field dependent molecular ionization model in [26-28] indicated that the model effectively captures the vast majorities of the physics associated with streamer development in transformer oil. Hence, the electric field dependent molecular ionization mechanism was considered as the source term of free charge carriers. Through laboratory investigation as well as numerical modeling [28-34], it has been shown that in dielectric liquids, impact and photo ionizations occur at electric field peaks of ~1×10^9 V/m leading to streamer propagation velocities of ~100 km/s. Such very high electric fields in dielectric liquids are not the case for the simulations presented in this paper. Therefore impact and photo ionizations are not considered in the model developed in this paper. Positive ion/electron recombination, positive/negative ion recombination and electron attachment phenomena represent the sink terms in the oil section. The solid portion of the WM DC mate-connector was modeled as a perfect insulator. The geometry of a WM DC connector containing oil-solid insulation subsystem located in a cylindrical electrode geometry was considered for primary simulations in [14].

After overcoming numerical solution issues including stabilization methods, meshing strategies and time steps [29], the accuracy of the model to achieve physically sound solutions was improved. In addition, a thermal diffusion equation was coupled to the model to capture the effect of the electrical power dissipation on the temperature of the oil. A needle-sphere electrode geometry with the electrodes covered by a dielectric solid and oil enclosed by the dielectric solid was considerd in [35]. This structure was used to conduct a fundamental study on effects of permittivity contrast/ difference of oil and dielectric solid on streamer propagation behavior in oil and electric field distribution in dielectric solid. It was shown that with the increase of the relative permittivity of the solid insulation, both the streamer average velocity in the oil and the electrical stress on the solid dielectric decease.

In this paper, the model developed in [35] is used to assess the influence of three parameters on streamer initiation. These three parameters are magnitude, rise time of applied voltage and the type of oil.

It should be noted that the model developed in this paper considers only deterministic attributes of streamers. However, besides deterministic factors, there are stochastic factors which lead to streamer branching. Stochastic causes of streamer branching, such as inhomogeneities inherited from noisy initial states, impurities and charge carrier density fluctuations can change the streamer velocity magnitude and direction [36]. Further research is needed to include stochastic factors in the model.

2 MATHEMATICAL MODEL

The set of equations for the time-dependent full thermo-electrodynamic modeling of the oil portion of a WM DC connector comprised of Poisson's equation, three charge continuity equations-one each for the positive and negative ions and one for the electrons-, and a thermal diffusion equation are as follows.

$$-\nabla\cdot(\epsilon_0\epsilon_{rl}\nabla V^l)=\rho_+^l+\rho_-^l+\rho_e^l\,,\quad \vec{E}^l=-\nabla V^l \quad (1)$$

$$\frac{\partial \rho_+^l}{\partial t} + \nabla \cdot \vec{J}_+^l = G_I\left(\left|\vec{E}^l\right|\right) + \frac{\rho_+^l \rho_e^l R_{+e}}{e} + \frac{\rho_+^l \rho_-^l R_\pm}{e}, \quad \vec{J}_+^l = \rho_+^l \mu_+ \vec{E}^l \quad (2)$$

$$\frac{\partial \rho_e^l}{\partial t} + \nabla \cdot \vec{J}_e^l = -G_I\left(\left|\vec{E}^l\right|\right) - \frac{\rho_+^l \rho_e^l R_{+e}}{e} - \frac{\rho_e^l}{\tau_a}, \quad \vec{J}_e^l = -\rho_e^l \mu_e \vec{E}^l \quad (3)$$

$$\frac{\partial \rho_-^l}{\partial t} + \nabla \cdot \vec{J}_-^l = \frac{\rho_e^l}{\tau_a} - \frac{\rho_+^l \rho_-^l R_\pm}{e}, \quad \vec{J}_-^l = -\rho_-^l \mu_- \vec{E}^l \quad (4)$$

$$\frac{\partial T^l}{\partial t} + \vec{v}^l \cdot \nabla T^l = \frac{1}{\rho_l^l c_v^l}\left(k_T^l \nabla^2 T^l + \phi_d^l\right) \quad (5)$$

where ρ_+^l, ρ_-^l and ρ_e^l are the densities of the positive ion charge, the negative ion charge and the electron charge in dielectric liquid, respectively. The negative ion and electron charge densities are both negative quantities. The sum of the right-hand sides of Equations (2)-(4) is zero due to charge conservation. Superscript "l" denotes that the variable exists in the liquid insulation. T^l is the temperature of the liquid in Kelvin, $\vec{v}^l$ is the velocity of the liquid, k_T^l is the thermal conductivity of the liquid, ρ_l^l is the liquid density, c_v^l is the specific heat of the liquid and ϕ_d^l is the dissipative source term. ϕ_d^l can be assumed to be purely electrical in nature and is the dot product of the current density and the local electric field, $\vec{E}^l.\vec{J}^l$, where

$$\vec{J}^l = \vec{J}_+^l + \vec{J}_-^l + \vec{J}_e^l = (\rho_+^l \mu_+ - \rho_-^l \mu_- - \rho_e^l \mu_e)\vec{E}^l \quad (6)$$

Here the liquid is assumed to not move with any notable velocity $\vec{v}^l = 0$ which is a reasonable assumption in the time frame considered for simulations in this paper

$G_I\left(\left|\vec{E}^l\right|\right)$ is charge density rate source term due to the process of molecular ionization in dielectric liquids such as transformer oil [26-28, 37]

$$G_I\left(\left|\vec{E}^l\right|\right) = \frac{e^2 n_0 a \left|\vec{E}^l\right|}{h} \exp\left(-\frac{\pi^2 m^* a \Delta^2}{e h^2 \left|\vec{E}^l\right|}\right) \quad (7)$$

where $e = 1.602 \times 10^{-19}\ C$ is the magnitude of electronic charge, $a = 3.0 \times 10^{-10}\ m$ is the molecular separation, $\left|\vec{E}^l\right|$ is the magnitude of the electric field in the liquid dielectric, $h = 6.626068 \times 10^{-34}\ m^2 kg/s$ is Planck's constant, $m^* = 0.1 m_e = 9.1 \times 10^{-32}\ kg$ is the effective electron mass in the liquid, Δ is the molecular ionization potential and n_0 is the number density of ionizable molecules.

Positive ion/electron recombination rate, R_{+e}, and positive/ negative ion recombination rate, $R_\pm$, are given by [26-28, 37]

$$R_{+e} = R_\pm = \frac{e(\mu_+ + \mu_-)}{\epsilon_0 \epsilon_{rl}} \quad (8)$$

where the mobility values of positive and negative ions are $\mu_+ = \mu_- = 1 \times 10^{-9} (\mathrm{m^2/V.s})$. $\epsilon_0 = 8.85 \times 10^{-12}\ F/m$ is the permittivity of vacuum and ϵ_{rl} is the oil relative permittivity. For transformer oil with $\epsilon_{rl} = 2.2$, $R_{+e} = R_\pm = 1.64 \times 10^{-17}\ \mathrm{m^3/s}$.

Electron attachment is modeled via an attachment time constant [38] with a value of $\tau_a = 200$ ns for transformer oil [26-28, 37].

The dielectric solid is modeled as a perfect insulator with zero conductivity ($-\nabla \cdot (\nabla V^s) = 0$). Therefore, the conduction current in the dielectric solid is zero, $\vec{J}^s = 0$, and the total current is only the displacement current. Superscript "s" denotes the variable in solid insulation. Due to the zero conductivity of the solid insulator, all volume charges (positive ion ρ_+^l, negative ion ρ_-^l, and electron ρ_e^l) in the liquid that travel to the interface are converted to a surface charge density ρ_s. Therefore, at the liquid-solid interface, an added governing equation accounts for the surface charge density ρ_s, whose time derivative is equal to the difference in normal conduction currents on either side of the interface

$$\frac{\partial \rho_s}{\partial t} = \vec{n} \cdot \left(\vec{J}^l - \vec{J}^s\right) = \vec{n} \cdot (\rho_+^l \mu_+ - \rho_-^l \mu_- - \rho_e^l \mu_e)\vec{E}^l \quad (9)$$

where $\vec{n}$ is the outward normal vector from the liquid side.

Based on Gauss' Law, the difference in normal displacement fields on either side of the interface is equal to the surface charge density

$$\rho_s = \vec{n} \cdot \left(\vec{D}^s - \vec{D}^l\right) \quad (10)$$

3 SIMULATION RESULTS AND DISCUSSION

Figure 1a shows a typical structure of a subsea DC connector comprising cable termination chambers and a WM DC chamber. Figure 1b shows the WM DC chamber in the unmated and mated positions. It can be seen that there are complicated solid-liquid insulation subsystems during its in-service work in the mated position.

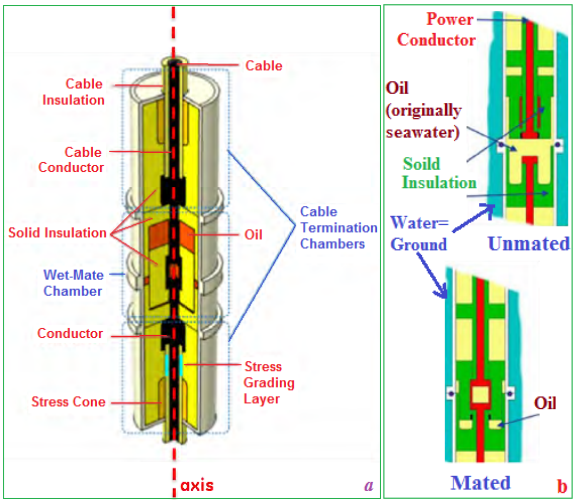

Figure 1. a) A typical structure of a subsea connector, b) WM connector in unmated and mated positions.

A solid-liquid model insulation system is considered to address the key challenges envisaged in a WM DC connector after mating, which includes a needle-sphere electrode geometry as described in IEC 60897 [39]. The electrodes are covered by a dielectric solid while transformer oil is enclosed by the dielectric solid as well. The dielectric solid considered

in this paper is epoxy ($\epsilon_r = 4.2$). The dielectric solid is a tubular structure oriented such that tube's inner radius surface is parallel to the direction of the main z-component of the electric field. This axial symmetry (2-D) drawn in COMSOL model is shown in Figure 2.

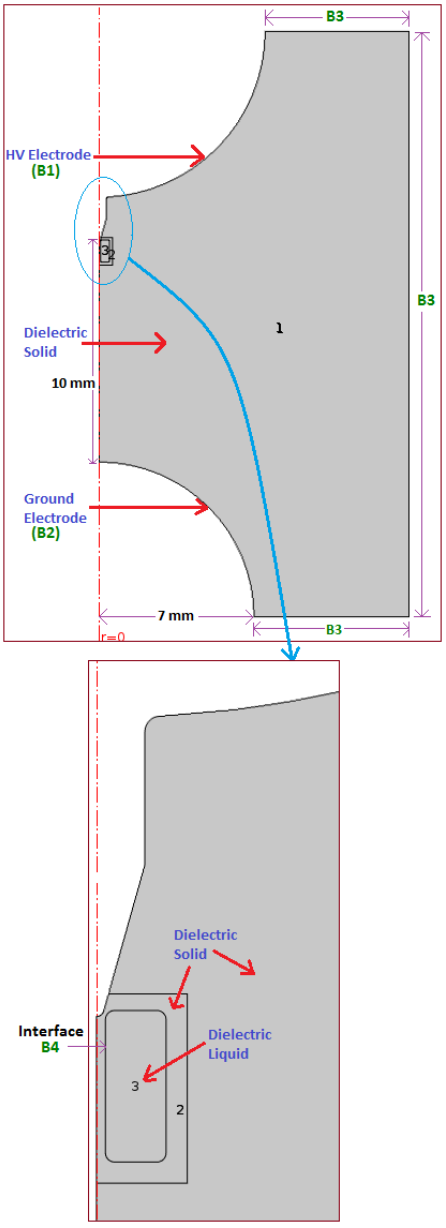

Figure 2. The needle-sphere electrode geometry and the insulation system.

The electrodes are 10 mm apart and the radii of curvature of the needle and sphere electrodes are 50 μm and 7.0 mm, respectively. These dimensions are different from those considered in [35].

To capture significant dynamics expected in the region surrounding the needle tip, a very dense mesh is needed. However, using this mesh for other regions with very large feature sizes compared to the needle tip demands very large memory resources and needs long simulation run-times.

To handle this difficulty, the area shown as region "2" in Figure 2 is defined, and the geometry is divided into three regions as follows. The regions "1" and "2" are the dielectric solid and the region "3" is the dielectric liquid. For regions "2" and "3", a dense domain mesh with a maximum element size of 3 μm is used while for region "1" a normal domain mesh is used. Also, for the needle tip, a part of the axial symmetry in region "2" as well as the solid-liquid interface, a very dense boundary mesh with maximum element size of 1 μm is used. The mesh strategy considered for the model has significant affects the simulation as discussed in [35].

Table 1 summarizes the boundary conditions considered for the geometry for all simulations in this paper. The HV electrode, ground electrode, insulation walls and dielectric solid-liquid interface are denoted as B1, B2, B3, and B4, respectively.

Table1. Boundary conditions.

Boundary	Electrostatics V	Transport of Charge Carriers (ρ_+, ρ_- and ρ_e)
B1	$V = V_{app}$	---
B2	$V = 0$	---
B3	Zero charge: $\vec{n}.\vec{D} = 0$	---
B4	$\rho_s = \vec{n} \cdot (\vec{D}^s - \vec{D}^l)$ $\frac{\partial \rho_s}{\partial t} = \vec{n}.(\rho_+^l \mu_+ - \rho_-^l \mu_- - \rho_e^l \mu_e)\vec{E}^l$	$\vec{n}.\vec{J}_+ = \begin{cases} \vec{n}.\vec{J}_+ & if\ \vec{n}.\vec{E} \geq 0 \\ 0 & if\ \vec{n}.\vec{E} < 0 \end{cases}$ $\vec{n}.\vec{J}_- = \begin{cases} \vec{n}.\vec{J}_- & if\ \vec{n}.\vec{E} \leq 0 \\ 0 & if\ \vec{n}.\vec{E} > 0 \end{cases}$ $\vec{n}.\vec{J}_e = \begin{cases} \vec{n}.\vec{J}_e & if\ \vec{n}.\vec{E} \leq 0 \\ 0 & if\ \vec{n}.\vec{E} > 0 \end{cases}$

The model used here to study streamer initiation and propagation was validated before in [35] with the verified simulation results reported in the literature.

3.1 THE INFLUENCE OF RISE TIME OF APPLIED VOLTAGE

In this section, the influence of rise time of applied voltage on streamer propagation pattern is investigated. Figure 3 shows the applied voltages considered: a) step voltage; b) step voltage with a rise time (defined as the time range from 10% to 90% of peak) of 10 ns; and c) step voltage with a rise time of 100 ns. The peak applied voltage is 300 kV.

According to the recommendations in [35], a small time step (Δt) of 1 ns is considered for all the simulations conducted in this paper to capture accurately the streamer dynamics in the oil portion. In all the simulations in this study, "*Consistent Stabilization*" methods are preferred for numerical solution stability. In the category of Consistent Stabilization, both "*streamline diffusion*" and "*crosswind diffusion through Codina algorithm*" techniques are considered as recommended in [35].

Figure 4 shows the rz-plane electric field magnitude distribution at t=50, 100, 150 and 200 ns for the three voltage waveforms shown in Figure 3 with different values of rise time. As shown in Figure 4, the shorter rise time, the more prominent streamer growth in the oil portion in the same period of time. When applying a voltage with a shorter rise time, the oil portion experiences higher electrical stress.

The movement of free charge carriers such as ions and electrons in the dielectric liquid can result in thermal dissipation.

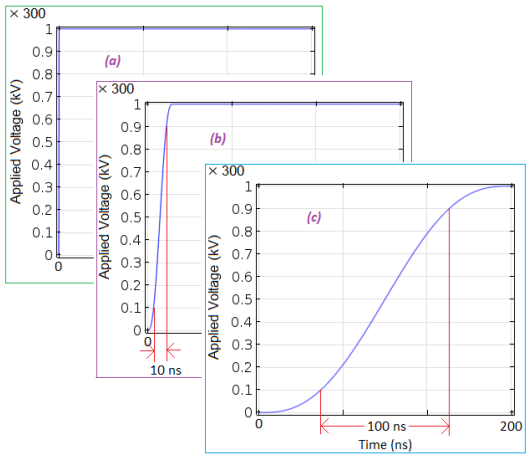

Figure 3. Three considered voltages with different rise times.

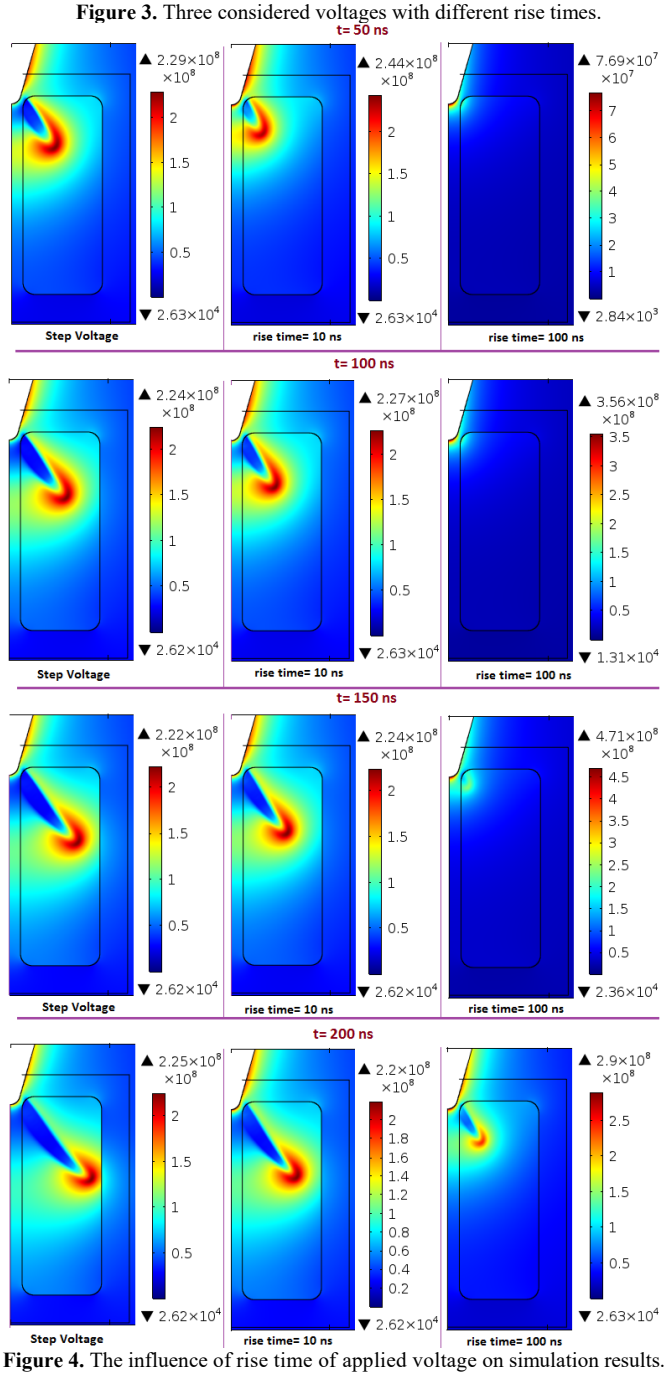

Figure 4. The influence of rise time of applied voltage on simulation results.

The effect of the electrical power dissipation on the temperature of the oil was modeled as a thermal diffusion process, as described in Eq.(5). In this regard, Figure 5 shows the rz- planeof temperature distribution in the oil at t=100 and 200 ns for the voltage waveforms applied with rise times of 10 and 100 ns. The initial temperature was considered at 300 K. It can be seen that at t=100 ns for the voltage with rise time of 100 ns, the oil temperature does not increase because the streamer growth in the oil at that time instance is negligible as shown in Figure 4.

However, for the voltage with rise time of 10 ns, the oil temperature increases to 312 K at t=100 ns. At t=200 ns, the area having a temperature higher than 300 K spreads further out than the cases with shorter rise time voltage waveforms. This result also comes to an agreement with the electric field magnitude distributions as shown in Figure 4.

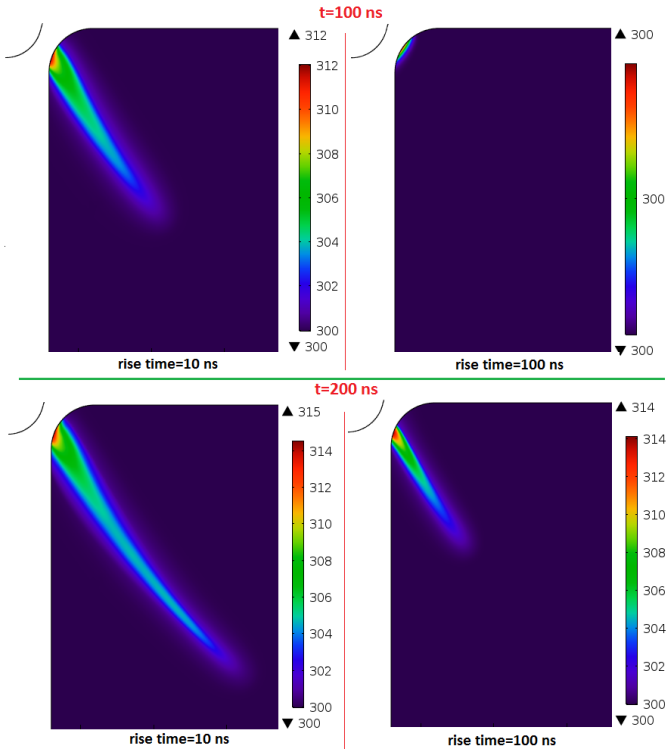

Figure 5. The rz-plane of temperature distribution in the oil at t=100 and 200 ns for the voltage applied with rise times of 10 and 100 ns.

3.2 THE INFLUENCE OF MAGNITUDE OF APPLIED VOLTAGE

In this section, the influence of magnitude of applied voltage on streamer propagation pattern is investigated. Three step voltages with amplitudes of 200, 300 and 400 kV are studied. Figure 6 shows the rz-plane electric field magnitude distribution at t=0, 25, 50, 75 and 100 ns. From Figure 6, it can be seen that:

- V_{app}=400 kV, i.e., $(8.24\times10^{8}$ V/m)×(400/200)= 1.65×10^{9} V/m. However, at later times, both the shape and the amplitude of the electric field distribution for three mentioned voltages are different.
- For V_{app}=200 kV, streamer growth is limited to only a small area in the corner of the oil portion as the glow discharge because of insufficient electric field magnitude in the oil

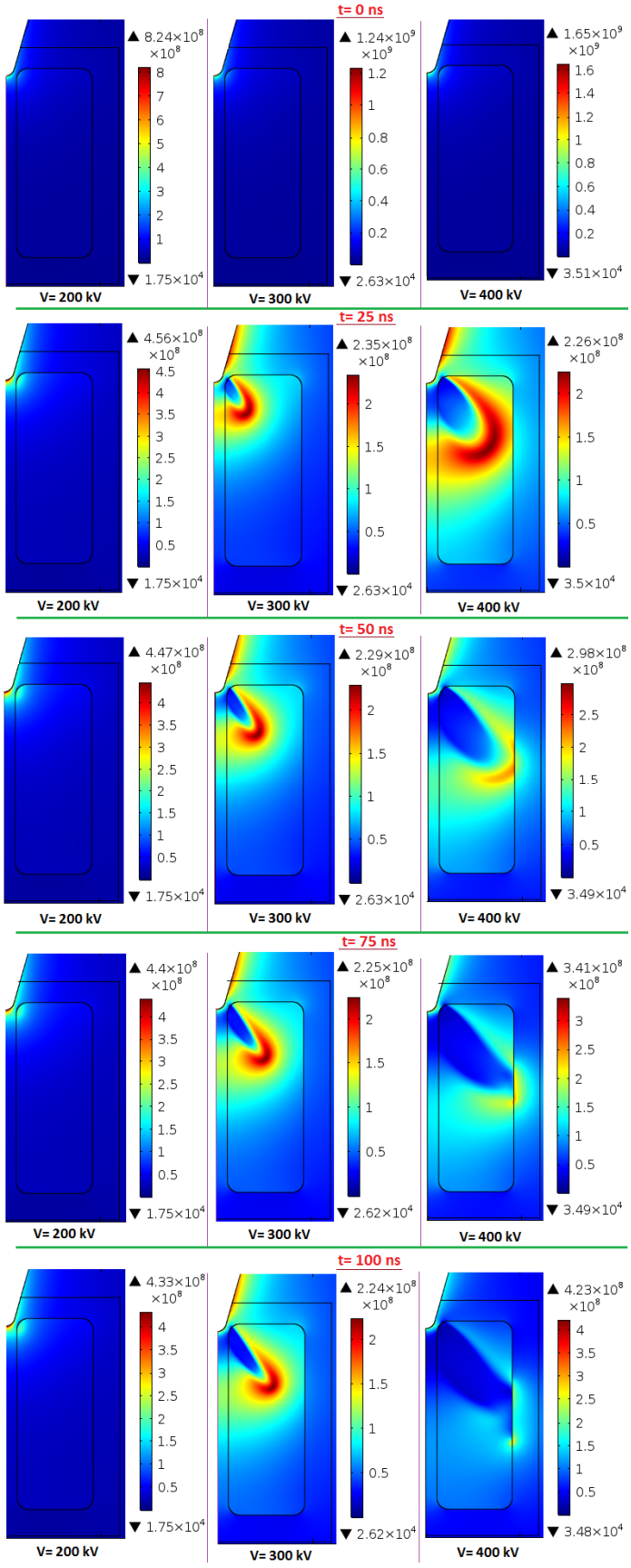

Figure 6. The influence of magnitude of applied voltage on simulation results.

portion, as shown in Figure 7a for t=100 ns. Figure 7a shows the electric field magnitudes along five parallel lines as marked in Figure 7b. From Figure 7a, it can be seen that the maximum electric field magnitude in the oil portion is less than 2×10^8 V/m which is insufficient to make significant streamers propagate.

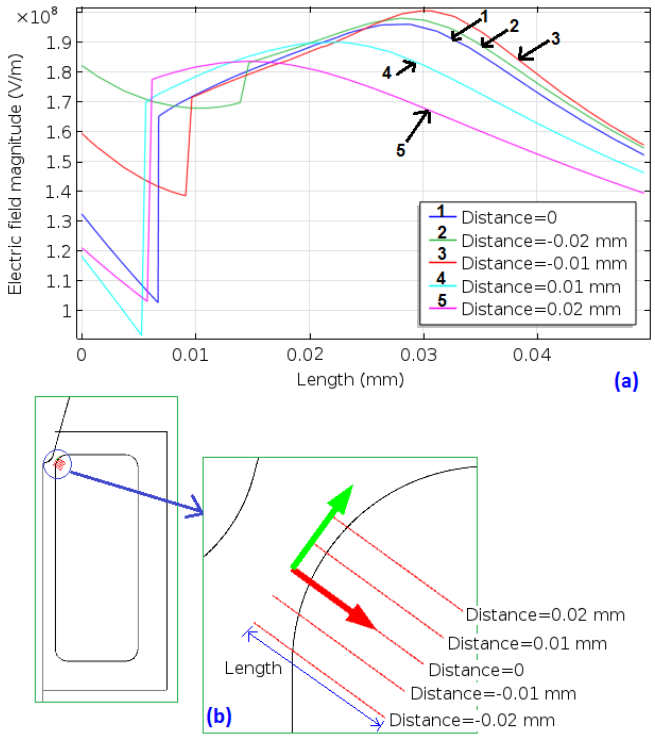

Figure 7. (a): Electric field magnitude along five parallel lines shown in (b).

- For V_{app}=300 kV, the electric field magnitude in the oil portion is sufficient to cause both radial r-direction and axial z-direction molecular ionization leading to the formation of a bubbly-like streamer (the snapshots at 25, 75 and 100 ns as shown in Figure 6). Figure 8 shows the electric field magnitude profile along the line denoted as AB at several time instances. The line starts from the HV electrode, passes through the dielectric solid and continues in the oil along the route experiencing the maximum electric field magnitude in the oil. According to Figure 8, the streamer velocity from t=25 ns to t=50 ns based on the electric field peaks at the mentioned time instances is 3 km/s. The electric field peak decreases from 2.35×10^8 V/m at t=25 ns to 2.29×10^8 V/m at t=50 ns. With the decease of the electric field peak to 2.25×10^8 V/m at t=75 ns, the streamer velocity for time between 50 ns and 75 ns also decreases to 2.2 km/s. This trend holds for later time instances, e.g., the streamer velocity for t=75 ns to t=100 ns also decreases to 1.8 km/s. In conclusion, a slight reduction in electric field magnitude e.g. only 2% from t=25 ns to t=100 ns in the oil leads to a notable reduction e.g. about 20% in the streamer velocity.

To describe the electric field magnitude profiles in the oil shown in Figures 6 and 8, net space charge density in the oil should be identified. Figure 9 shows the positive ion (ρ_+^l), negative ion (ρ_-^l), electron (ρ_e^l) and net space charge ($\rho_t^l = \rho_+^l + \rho_-^l + \rho_e^l$) densities in the oil along the line AB as shown

in Figure 8 at different time instances. From Figure 9, it can be seen that:

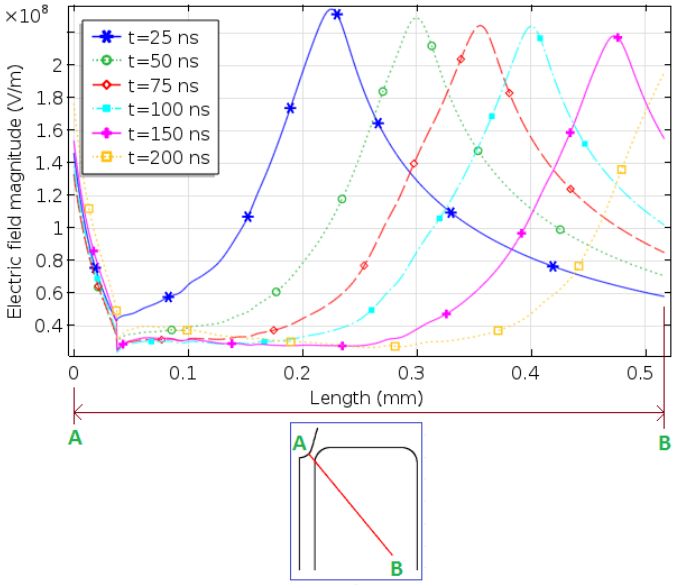

Figure 8. Electric field magnitude profile along the line denoted as AB at several time instances.

a. A net space charge density travels along the line AB leading to a traveling electric field wave shown in Figures 6 and 8.

b. The polarity of net space charge density is positive. The molecular ionization process results in the generation of the electrons and the positive ions. Since the mobility of the electrons is five orders of magnitude greater than that of the positive ions ($\mu_e = 10^5\mu_+$), the generated electrons depart from the streamer head quickly toward the interface portion close to the positive HV electrode and convert to surface charges. At the same time the positive ions are almost motionless. Therefore, net space charge density in the oil is generally positive in particular at the streamer head where a high electric field zone forms. Negative ions are generated by the attachment mechanism when the electrons generated by molecular ionization mechanism are traveling from the streamer head towards the positive needle HV electrode. Hence as seen in Figure 9, negative ion densities at different time instances are smaller than positive ion and electron densities.

- For V_{app}=400 kV, the electric field magnitude in the oil is higher than that for V_{app}=300 kV. Therefore, at t=25 ns, streamers propagate over a much greater area in the oil as shown in Figure 6. For V_{app}=300 kV, despite the nearly same peaks of net space charge density at different time instances as seen in Figure 9, the electric field peaks decrease slightly over time. This is because the electric field intensity anywhere in the oil at any time instance is resulted from an external electric field due to the voltage applied to the needle HV electrode as well as space charges. The farther away from the needle HV electrode, the less the electric field magnitude becomes. For V_{app}=400 kV the above trend is valid until the streamer head intersects the interface at t=40 ns. Afterwards, the radial r-direction movement of streamers is inhibited by the interface, leading to the accumulation of positive net space charge near the interface. This causes electric field magnitudes to increase over time, e.g. for t=50, 75 and 100 ns as shown in Figure 6.

3.3 THE INFLUENCE OF THE TYPE OF OIL

Recirculated from one position to another, a liquid makes it possible the movement of a metal contact for the purpose of mating or de-mating electrically a WM connector. Since, in such design, the liquid will be part of the insulation system of a WM connector after mating, insulating oil e.g. transformer oil should be used. In general, transformer oil is mainly a mixture of three types of hydrocarbon molecules including aromatics (C_nH_n), naphthenics ($C_{2n}H_{2n}$) and paraffinics ($C_{2n}H_{2n+2}$) where their composition and concentration depend on manufacturer and petroleum source [40].

In this regard, the influence of the type of oil on the model is reflected in $G_I(|\vec{E}^l|)$ in Eq. (7) through two parameters: (a) number density of ionizable molecules (n_0), and (b) molecular ionization potentials (Δ). In commercial transformer oil, aromatic molecules have both lower Δ value and lower n_0 value than naphthenic/paraffinic molecules.

For aromatics, $n_0 = 1 \times 10^{23}\text{m}^{-3}$ and Δ= 6.2 eV and for naphthenics/paraffinics $n_0 = 1 \times 10^{25}\text{m}^{-3}$ and Δ= 9.86 eV are considered [28, 41-42]. All simulation results presented in Figures 4-9 are for WM connectors with insulating oil comprising only aromatics.

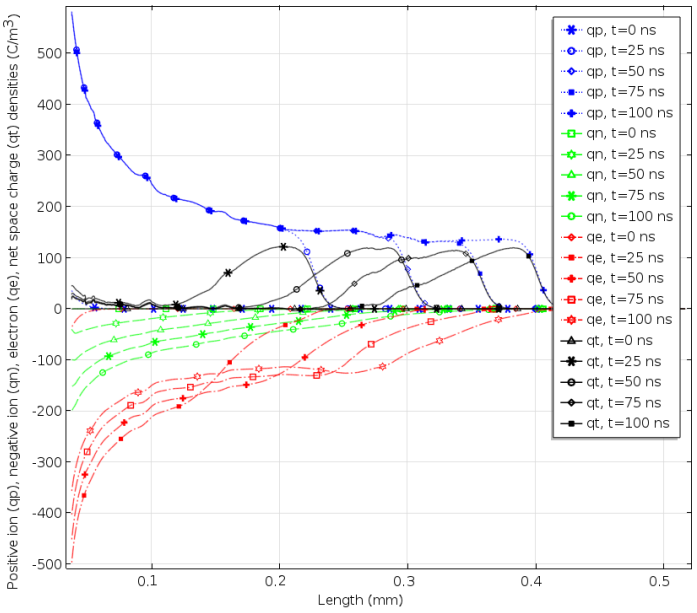

Figure 9. Positive ion, negative ion, electron, and net space charge densities in the oil along the line AB shown in Figure 8 at different time instances.

Figure 10 shows the rz-plane electric field magnitude distribution at different time instances under 300 kV step voltages for two cases: (a) "Oil #1" includes only aromatics, and (b) Oil #2 includes only naphthenics/paraffinics. The results for "Oil #1" was presented before in Figure 6 and repeated in Figure 10 for comparison with the results for "Oil #2" case. For "Oil #2" case, the maximum electric field magnitude shown in Figure 10 at t=25, 50, 75 and 100 ns is

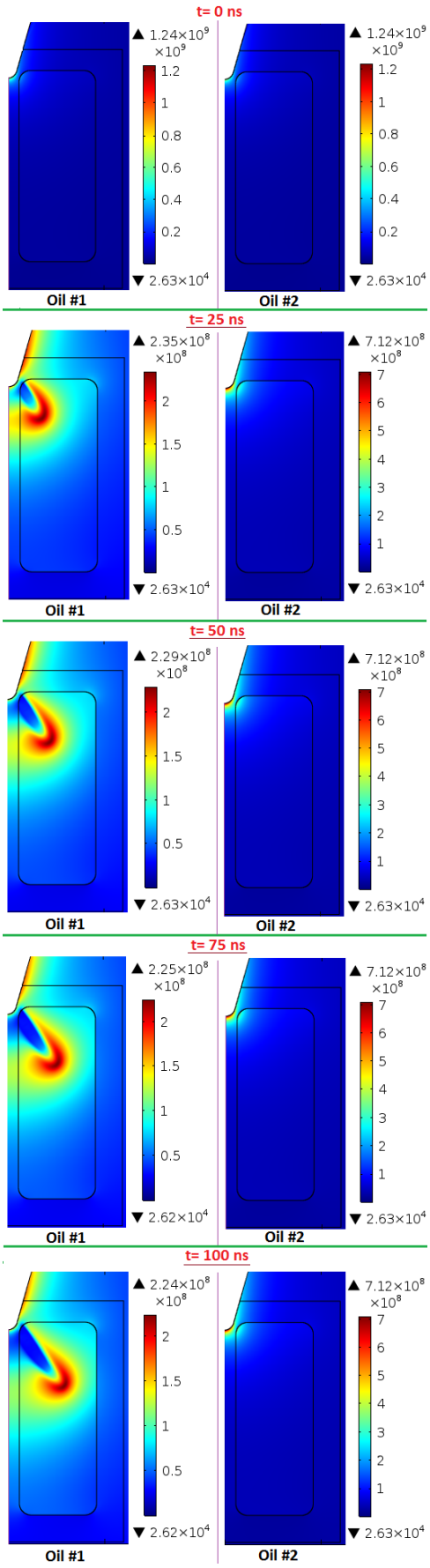

Figure 10. The rz-plane electric field magnitude distribution at different time instances for two types of oil, (Vp=300 kV).

7.12×10^8 V/m which occurs close to the needle tip in the dielectric solid. However, the maximum electric field magnitude in the oil portion not shown here is about $3\text{-}3.2\times10^8$ V/m. Despite a sufficiency of this value to grow streamers in aromatics, it leads to only glow discharge in naphthenics/paraffinics.

The n_0 value for aromatics is two orders of magnitude less than that of naphthenics/paraffinics. However due to lower molecular ionization potential, aromatics lead to significant streamer growth and propagation for V_p=300 kV while for naphthenics/paraffinics, streamers are not well initiated.

Figure 11 shows the simulation results under V_p=400 kV for two types of oil. Under this voltage, the maximum electric field magnitude in "Oil #2" reaches about 4×10^8 V/m which is still insufficient to propagate streamers. With increasing the applied voltage to 450 kV, streamers grow and propagate in "Oil #2", as shown in Figure 12. Figure 13 shows the electric field magnitude profile along the line denoted as AB (as shown in Figure 8 at several time instances).

From Figure 13, it can be seen that the streamer velocity is about 0.42 km/s until t=100 ns and then increases gradually to 1 km/s until t=200 ns. The electric field peak value increases from 4.36×10^8 V/m at t=25 ns to 5×10^8 V/m at t=200 ns. The trend of streamer velocity and electric field shown in Figure 13 for naphthenics/paraffinics is in the opposite direction to those in Figure 8 for aromatics. A higher value of Δ for naphthenics/paraffinics causes a higher inception electric field for streamer initiation. However, if streamers are initiated, a higher value of n_0 generates more charge carriers at the streamer head and consequently leads to the increase of the electric field peak value and the streamer velocity over time for naphthenics/paraffinics, as compared to aromatic. In order to assess the influence of n_0, the case of Figure 12 is run for $n_0 = 1\times10^{23}\mathrm{m}^{-3}$ where Figure 14 shows its rz-plane electric field magnitude distribution and the electric field magnitude profile along the line, denoted as AB, at several time instances. From Figure 14 it can be seen that in spite of an electric field magnitude higher than 4.5×10^8 V/m in the oil portion, it does not lead to the streamer growth and propagation. This clearly demonstrates the key role of n_0 during the processes of streamer initiation and propagation.

The findings in this section as well as in sections 3.1 and 3.2 show that aromatics need an electric field magnitude larger than 2×10^8 V/m to cause streamers to propagate. This value is 4×10^8 V/m for naphthenics/paraffinicsis as shown in this section. These values as well as the streamer velocities reported in this paper are in good agreement with experimental investigations and numerical simulations reported in [26-28, 30, 32, 43-44].

Since streamers are denoted as the underlying cause of breakdown in a dielectric liquid, identifying factors to prevent the streamer growth and propagation is extremely important. Based on the simulation results presented in this section, it is recommended to use the dielectric oil with molecular constituents having high molecular ionization potentials e.g. naphthenics and paraffinics and minimize the use of molecules having low molecular ionization potentials e.g. aromatics for

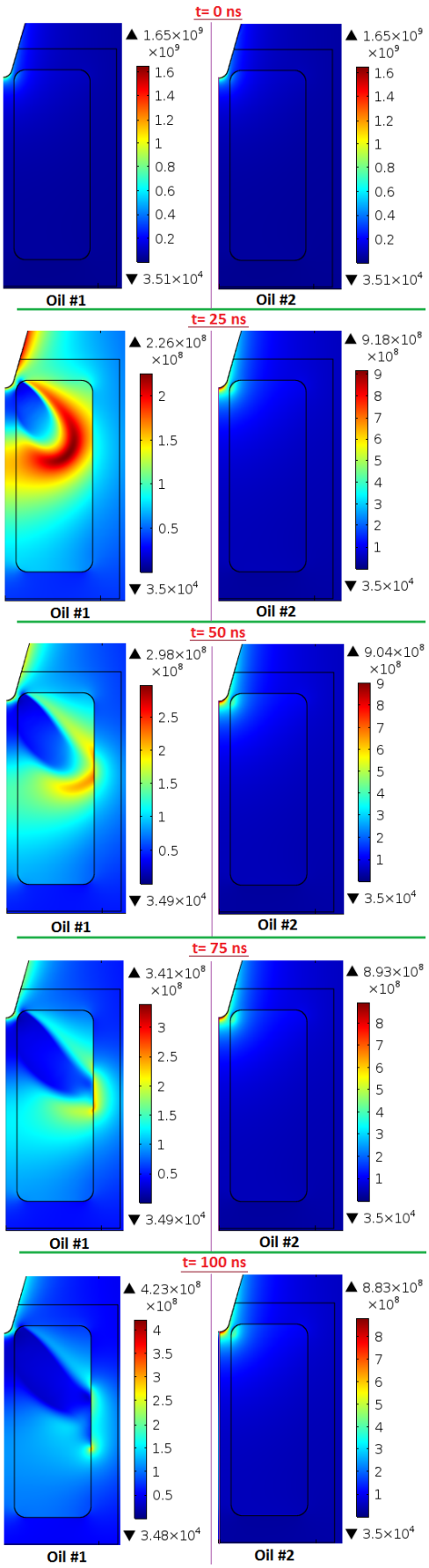

Figure 11. The rz-plane electric field magnitude distribution at different time instances for two types of oil, (Vp=400 kV).

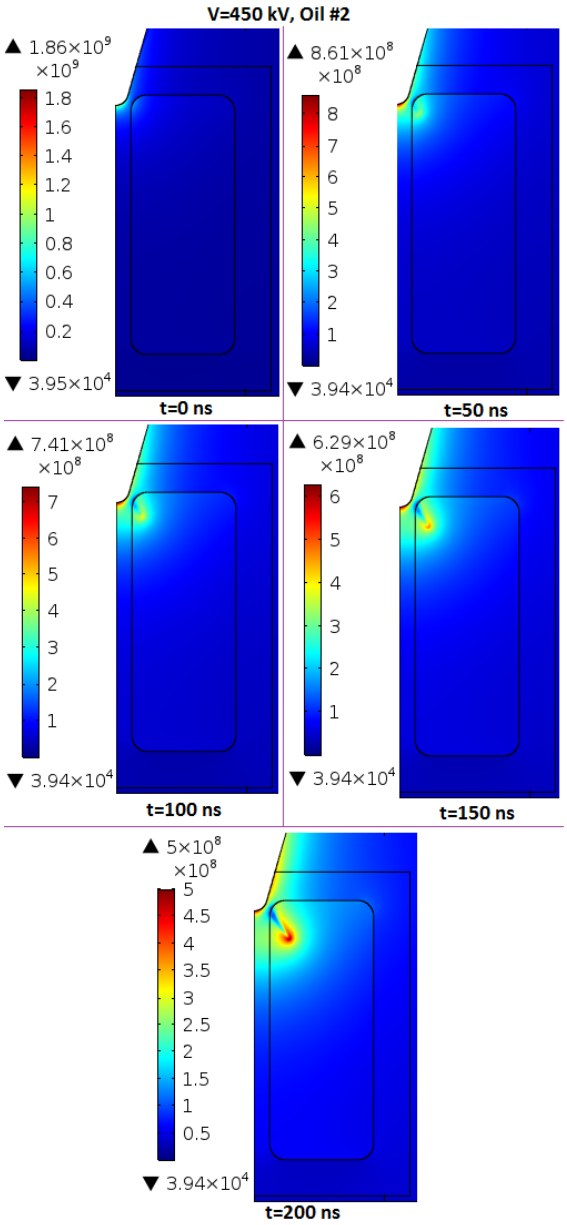

Figure 12. The rz-plane electric field magnitude distribution at different time instances for "Oil #2", (Vp=450 kV).

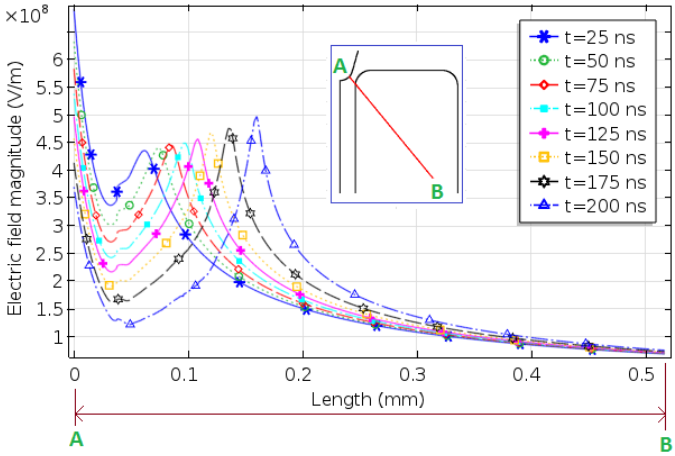

Figure 13. Electric field magnitude profile along the line denoted as AB at several time instances for "Oil #2" type under V_p=450 kV.

WM DC connectors. By using these findings and the model of this paper, an engineering study can be conducted on the streamer propagation behavior of various commercial mineral oils, synthetic esters, fluorocarbon-based oils, vegetable-based oils and nanofluid oils in a cylindrical geometry of a WM DC connector. It is believed that the type of oil holds the key to achieve compact designs of WM DC chambers when dealing with switching transients. It should be noted that in commercial transformer oil there are both the trace aromatic molecules and the main high density naphthenic (or paraffinic) molecules. Therefore further research on developing a two species model to include both molecular species is needed.

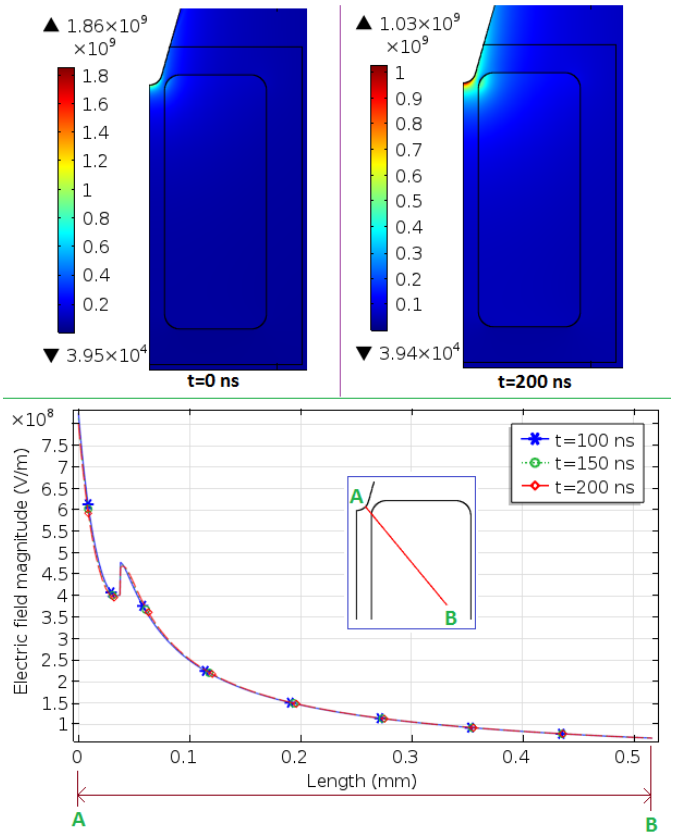

Figure 14. The rz-plane electric field magnitude distribution at different time instances "Oil #2" with $n_0 = 1 \times 10^{23}\mathrm{m}^{-3}$, (Vp=450 kV).

Residual moisture and ions in the dielectric liquid of a WM DC connector may affect streamer initiation and propagation features. The aging of dielectric oil is another serious threat to a WM connector which is expected to have the highest level of integrity for long life. To include these complicated issues in the model, some parameters e.g. Δ and n_0 which may be impurity-dependent should be determined experimentally. Moreover experimental research should be conducted on the influence of impurities on characteristics of streamer propagation in the dielectric liquid employed in a WM connector. Further research is needed to address these issues.

4 CONCLUSIONS

By using the time-dependent full thermo-electrodynamic model developed in this paper, the influence of magnitude and rise time of applied voltage as well as the type of oil on the streamer propagation in the oil portion was investigated. The model includes the equations for the dielectric solid portion and solid-liquid interface to simulate the complicated solid-liquid insulation system of a WM DC chamber. It was found that fast transients having smaller rise time cause streamers to initiate sooner and propagate over greater areas. The polarity of net space charge density is positive. Due to the molecular ionization process and greater mobility of electrons compared to positive ions, the polarity of net space charge density is positive. The number density of ionizable molecules (n_0) and molecular ionization potential (Δ) which define the type of oil in the model, play key roles during the processes of streamer initiation and propagation. Aromatics need an electric field magnitude larger than 2×10^8 V/m to cause streamers to propagate while this value is 4×10^8 V/m for naphthenics/ paraffinicsis. Using compounds with higher molecular ionization potentials prohibits the streamer initiation and propagation in the oil.

ACKNOWLEDGMENT

Funding for this work is provided by RPSEA through the "Ultra-Deepwater and Unconventional Natural Gas and Other Petroleum Resources" program authorized by the U.S. Energy Policy Act of 2005. RPSEA (www.rpsea.org) is a nonprofit corporation whose mission is to provide a stewardship role in ensuring the focused research, development, and deployment of safe and environmentally responsible technology that can effectively deliver hydrocarbons from domestic resources to the citizens of the United States. RPSEA, operating as a consortium of premier U.S. energy research universities, industry, and independent research organizations, manages the program under a contract with the U.S. Department of Energy's National Energy Technology Laboratory.

REFERENCES

[1] R.S. Zhang, R. Datta, C.M. Sihler and M.J. Song, "Modular stacked subsea power system architectures," U.S. Patent No. 8692408, April 2014.
[2] D. Dong, R. Lai, S. Chi, R.K. Gupta and D. Zhang, "Method and system for architecture, control, and protection systems of modular stacked direct current subsea power system," U.S. Patent No. 9178349, Nov. 2015.
[3] General Electric Global Research Report, *MSDC Electrical System for Deepwater Subsea Process*, Contract No. 08121-2901-01, Nov. 2013.
[4] T. Hazel, H.H. Baerd, J.J. Legeay and J.J. Bremnes, "Taking power distribution under the sea: design, manufacture, and assembly of a subsea electrical distribution system," IEEE Industry Applications Mag., Vol. 19, No.5, pp. 58-67, 2013.
[5] GE Vetco Gray, *MECON WM-I and II*, Product Information Sheet.
[6] GE Vetco Gray, *MECON DM-I, II and III*, Product Information Sheet.
[7] https://www.youtube.com/watch?v=UilBwGRODcI
[8] GE Global Research Report, *Subsea High Voltage Direct Current Connectors for Environmentally Safe and Reliable Powering of UDW Subsea Processing*, Contract No.12121-6302-01, 2015.
[9] CIGRE WG 21.02, Recommendations for tests of power transmission DC cables for rated voltage up to 800 kV, Electra No. 189, pp. 39-55, April 2000.
[10] CIGRE WG B1.32, Recommendations for testing DC extruded cable systems for power transmission at a rated voltage up to 500 kV, Technical Brochure 496, April 2012 (replace the TB 219).
[11] IEC 62895 "HVDC power transmission cables with extruded insulation and their accessories for rated voltages up to 320 kV for land applications–Test methods and requirements", (under preparation).
[12] GE Global Research Report, *Mock-up Subsea HVDC Connectors Bench-scale Test Procedures*, Contract No.12121-6302-01, April 2015.

[13] R. Smeets, "Safe-guarding the supergrid," IEEE Spectrum, Vol. 52, No. 12, pp. 38-43,Dec. 2015.
[14] M. Ghassemi, M. B. Tefferi, Q. Chen and Y. Cao, "Modeling a liquid-solid insulation system used in a dc wet-mate connector", IEEE Conf. Electr. Insul. Dielectr. Phenomena, Toronto, Canada, pp. 161-166, 2016.
[15] R.H. Fowler and L. Nordheim, "Electron Emission in Intense Electric Fields," Proc. Roy. Soc. A, Vol. 119, No. 781, pp. 173-181, 1928.
[16] L. Nordheim, "The effect of the image force on the emission and reflection of electrons by metals," Proc. Roy. Soc. A, Vol. 121, No. 788, pp. 626-639, 1928.
[17] C.A. Spindt, I. Brodie, L. Humphrey and E.R. Westerberg, "Physical properties of thin-film emission cathodes with molybdenum cones," J. Appl. Phys., Vol. 47, pp. 5248-5263, 1976.
[18] L. Onsager, "Deviations from Ohm's law in weak electrolytes," J. Chem. Phys., Vol. 2, pp. 599-615, 1934.
[19] A. Alj, A. Denat, J.P. Gosse, B. Gosse, "Creation of charge carriers in nonpolar liquids," IEEE Trans. Electr. Insul., Vol. 20, pp. 221-231, 1985.
[20] U. Gafvert, A. Jaksts, C. Tornkvist, L. Walfridsson, "Electrical field distribution in transformer oil," IEEE Trans. Electr. Insul., Vol. 27, pp. 647-660, 1992.
[21] F. Pontiga and A. Castellanos, "Electrical conduction of electrolyte solutions in nonpolar liquids," IEEE Trans. Indus. Appl., Vol. 32, No. 4, July/August 1996.
[22] J.C. Devins, S.J. Rzad and R.J. Schwabe, "Prebreakdown phenomena in liquids: electronic processes," J. Phys. D: Appl. Phys., Vol. 9, L87-91, 1976.
[23] J.C. Devins, S.J. Rzad and R.J. Schwabe, "Breakdown and pre-breakdown phenomena in liquids," J. Appl. Phys., Vol. 52, No. 7, pp. 4531-4545, July 1981.
[24] W.G. Chadband, "On variations in the propagation of positive discharges between transformer oil and silicone fluids," J. Phys. D: Appl. Phys., Vol. 13, pp. 1299-1307, 1980.
[25] F. O'Sullivan, S.H. Lee, M. Zahn, L. Pettersson, R. Liu, O. Hjortstam, T. Auletta, U. Gafvert, "Modeling the effect of ionic dissociation on charge transport in transformer oil," IEEE Conf. Electr. Insul. Dielectr. Phenomena (CEIDP), Kansas City, MO, USA, pp. 756-759, 2006.
[26] F. O'Sullivan, *A model for the Initiation and Propagation of Electrical Streamers in Transformer Oil and Transformer Oil based Nanofluids*, Ph.D. dissertation, MIT, Cambridge, MA, 2007.
[27] F. O'Sullivan, J.G. Hwang, O. Hjortstam, L. Pettersson, P. Biller, "A model for the initiation and propagation of positive streamers in transformer oil," IEEE Int'l. Sympos. Electr. Insul. (ISEI), Vancouver, BC, Canada, pp. 210-214, 2008.
[28] J.G. Hwang, *Elucidating the Mechanisms behind Prebreakdown Phenomena in Transformer Oil systems*," Ph.D. dissertation, MIT, Cambridge, MA, 2010.
[29] Yu. V. Torshin, "On the existence of leader discharges in mineral oil," IEEE Trans. Dielectr. Electr. Insul., Vol. 2, No. 1, pp. 167-179, 1995.
[30] L. Lundgaard, D. Linhjell, G. Berg, and S. Sigmond, "Propagation of positive and negative streamers in oil with and without pressboard interfaces," IEEE Trans. Dielectr. Electr. Insul., Vol. 5, No. 3, pp. 388-395, 1998.
[31] O. Lesaint and G. Massala, "Positive streamer propagation in large oil gaps: experimental characterization of propagation modes," IEEE Trans. Dielectr. Electr. Insul., Vol. 5, No. 3, pp. 360-370, 1998.
[32] D. Linhjell, L. Lundgaard, and G. Berg, "Streamer propagation under impulse voltage in long point-plane oil gaps," IEEE Trans. Electr. Insul., Vol. 1, No. 3, pp. 447-458, 1994.
[33] R. Liu, C. Tornkvist, V. Chandramouli, O. Girlanda, and L. A. A. Pettersson, "Ester fluids as alternative for mineral oil: the difference in streamer velocity and LI breakdown voltages," IEEE Conf. Electr. Insul. Dielectr. Phenomena (CEIDP), Virginia Beach, VA, USA, pp. 543-548, 2009.
[34] R. Badent, "Streamer model based on electronic processes in liquids," IEEE Conf. Electr. Insul. Dielectr. Phenomena (CEIDP), Vol. 2, Austin, TX, USA, pp. 447-450, 1999.
[35] M. Ghassemi, M. B. Tefferi, Q. Chen, and Y. Cao, "Positive streamer propagation in a wet-mate dc connector", IEEE Trans. Dielectr. Electr. Insul., Vol. 24, pp. 905-918, 2017.
[36] V. Y. Ushakov, V. F. Klimkin, and S. M. Korobeynikov, *Impulse Breakdown of Liquids*," Springer-Verlag, Berlin, 2007.
[37] J. Qian, R.P. Joshi, E.Schamiloglu, J. Gaudet, J.R. Woodworth and J. Lehr, "Analysis of polarity effects in the electrical breakdown of liquids," J. Phys. D: Appl. Phys., Vol. 39, pp. 359-369, 2006.
[38] W.F. Schmidt, "*Liquid State Electronics of Insulating Liquids*," CRC Press, pp. 121-123, 1997.
[39] IEC 60897:1987, *Methods for the determination of the lightning impulse breakdown voltage of insulating liquids*.
[40] M. Khalifa, editor. *High-Voltage Engineering: Theory and Practice,* Second Edition, Marcel Dekker Inc., New York, 2000.
[41] P. Biller, "A simple qualitative model for the different types of streamers in dielectric liquids," IEEE 12th Int'l. Conf. Conduction and Breakdown in Dielectric Liquids (ICDL 1996), Rome, Italy, pp.189-192, 1996.
[42] H. S. Smalo, P.O. Astrand, and S. Ingebrigtsen, "Calculation of ionization potentials and electron affinities for molecules relevant for streamer initiation and propagation," IEEE Trans. Dielectr. Electr. Insul., Vol. 17, No. 3, pp. 733-741, 2010.
[43] R. Liu, A. Jaksts, and T. Bengtsson, "Streamer propagation in composite oil/cellulose insulation under LI voltages," International Symposium on Electrical Insulation (ISEI), Anaheim, CA, USA, pp. 426-430, 2000.
[44] R. Liu and A. Jaksts, "Breakdown processes in transformer insulation under li voltages," International Conference on Dielectric Liquids (ICDL), Coimbra, Portugal, pp. 75-78, 2005.

Mona Ghassemi (S'07-M'13-SM'16) was graduated with a BS in electrical engineering from Shahed University in Tehran, Iran in 2004 and received her MS and PhD degrees both with the first honor in electrical engineering from the University of Tehran, Iran in 2007 and 2012, respectively. She spent two years researching as a postdoctoral fellow at NSERC/Hydro-Quebec/UQAC Industrial Chair on Atmospheric Icing of Power Network Equipment (CIGELE) and Canada Research Chair on Power Network Atmospheric Icing Engineering (INGIVRE), University of Quebec at Chicoutimi (UQAC), QC, Canada from 2013 to 2015. Since 2015, she has been a postdoctoral fellow at the Electrical Insulation Research Center (EIRC) of Institute of Materials Science (IMS) at the University of Connecticut. Her research interests are in dielectrics, electrical insulation materials and systems, high voltage technology, plasma science and computation of electromagnetic transients in power systems. She is a registered Professional Engineer in the Province of Ontario, Canada.

Qin Chen is a Senior Electrical Engineer at GE Global Research, where he has been working since 2008. His background is in dielectric materials and electrical insulation systems. His recent work focuses on the development of high-voltage direct current (HVDC) components, such as subsea DC connectors, extruded HVDC cables, and HVDC converter transformers. His interest also includes the development of new polymeric and nanocomposite DC insulation materials, as well as the fundamental study of polarization and electrical charge transport in dielectric materials using both experimental and multi-physics modeling techniques. Besides HVDC systems, his other experiences include the development of high energy density dielectric materials for energy storage film capacitors, design of AC transformers, monitoring and diagnostics of power instruments, and the study of ferroelectric polymers and developing electro-optical devices based on these materials. Qin received his BS degree from Tsinghua University (Beijing, China) in 2003, and his MS and PhD degrees from Penn State University in 2006 and 2008, all in Electrical Engineering.

Yang Cao was graduated with BS and MS in physics from Tongji University in Shanghai, China, and received his PhD from the University of Connecticut in 2002, after which he served as a senior electrical engineer at GE Global Research Center. Since 2013, he has been an associate professor at the Electrical and Computer Engineering Department of the University of Connecticut. His research interests are in the physics of materials under extreme electric field and the development of new dielectric materials, particularly the polymeric nanostructured materials, for energy-efficient power conversion and renewables integrations, as well as for novel medical diagnostic imaging devices.